Lidar-Assisted Control for Wind Turbines I

Prof. Dr.-Ing. David Schlipf

09.09.2024

Lecture #10 of Course
“Controller Design for Wind Turbines and Wind Farms”

Hochschule Flensburg
University of Applied Sciences

SWE Stuttgart Wind Energy
@ Institute of Aircraft Design

Wind Energy Technology Institute

Schedule

02.09.	1	Controller Design Objectives and Modeling
03.09.	2	Baseline Generator Torque Controller
04.09.	3	Collective Pitch Controller
05.09.	4	Filter Design
06.09.	7	Wind Field Generation
09.09.	10	Lidar-Assisted Control I
10.09.	11	Lidar-Assisted Control II
11.09.	5	Tower Damper
12.09.	6	Advanced Torque Controller
12.09.	8	Steady State Calculations
16.09.	9	Individual Pitch Control
17.09.	12	Wind Farm Effects
18.09.	13	Wind Farm Control
19.09.	14	Floating Wind Control I
20.09.	15	Floating Wind Control II

Lidar-Assisted Control for Wind Turbines

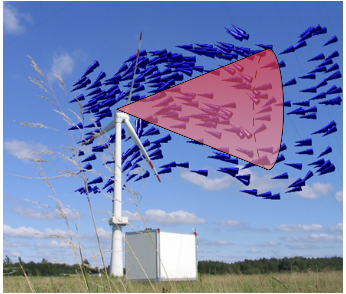

Motivation

- wind is changing over space and time
- conventional control reacts after impact
- lidar technology provides wind preview
- better control performance is expected

Main questions

- How can useful wind preview signals be extracted from lidar data?
- How can these signals be used to improve wind turbine control?

Contents

Introduction to Lidar

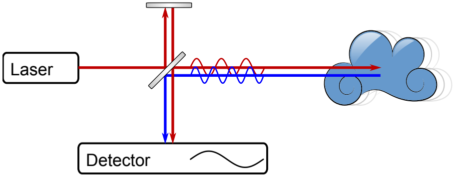

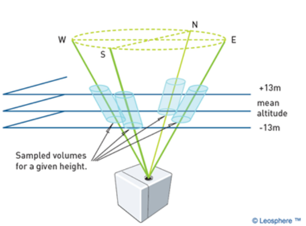

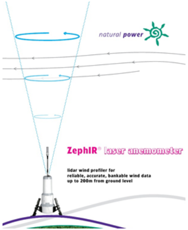

LIght Detection And Ranging

- uses optical Doppler effect
- measures speed of aerosols

Commercial development

- since around 2003 popular for site assessment purposes
- based on components from telecommunications
- typical 10 min average of wind direction and horizontal speed
- price similar to met mast
- pulsed and continuous wave

Optical Doppler Effect

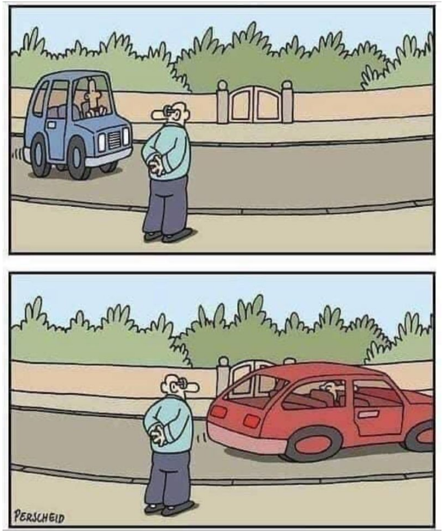

Lidar Data Processing

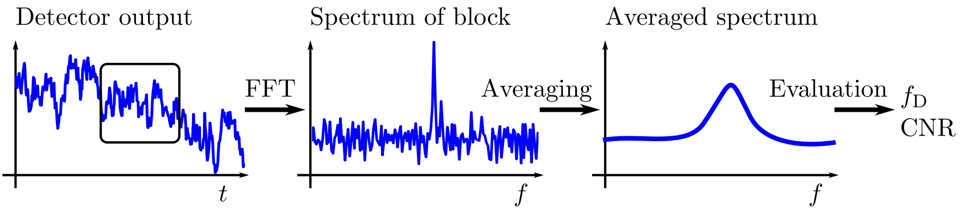

- Frequency shift f_D can be translated into a line-of-sight wind speed by $v_\mathrm{los} = \frac{c f_\mathrm{D}}{2 f_\mathrm{L}}$, where c is speed of light and f_L is the frequency of the emitted light.
- Due to FFT and pulse length (pulsed lidar) or spatial sensitivity (continuous wave), measurement is in volume and not in a point.
- Carrier-to-noise (CNR) provides a quality signal for the measurement.

Most Common Offshore Lidar Systems

[www.zxlidars.com]

[www.vaisala.com]

Most Common Nacelle-based Lidar Systems

[www.zxmeasurements.com]

[www.windarphotonics.com]

[Vamos Project]

[WETI]

Comparison of Continuous-wave and Pulsed Lidar

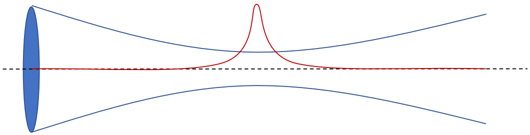

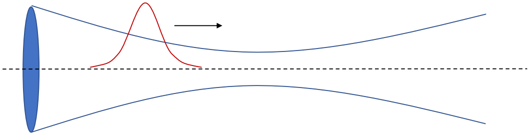

Continuous-wave lidar

- ZX, Windar
- Low minimum range (ZX, 10 m) and short probe length close to turbine
- High sensitivity, independent of range
- Very rapid measurement rates

Pulsed lidar

- Leosphere, Molas
- Greater maximum range (limited only by signal strength)
- Near-constant probe length
- Ranges acquired in parallel

Components of Continuous-wave and Pulsed Lidar

MAIN COMPONENTS OF A CW WIND LIDAR

- Laser
  - Provides source of light with special characteristics
- Telescope
  - Transmits the light beam & receives the return signal
- Scanner
  - Directs the beam to a chosen location **or** at a chosen angle
- Detector
  - Converts returning light signals (photons) to voltage/current (electrons)
- Digital signal processing
  - Converts analogue detector O/P to digits and crunches the numbers

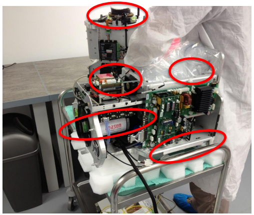

[M.Harris, Introduction to cw doppler lidar]

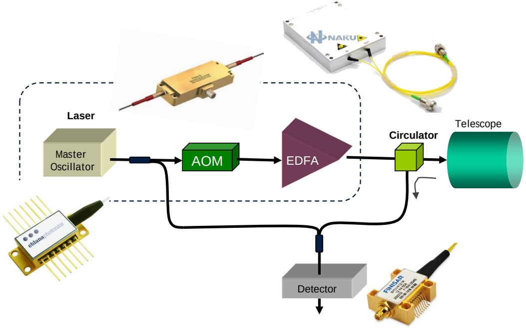

[P. Rosenbusch, Pulsed lidar for remote wind sensing]

Wind Disturbance Modeling

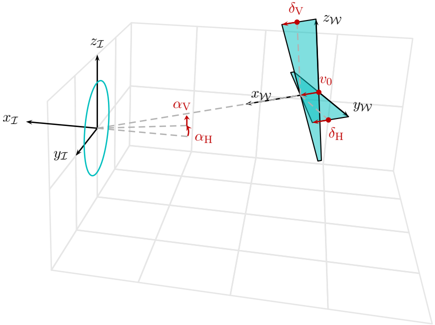

Realistic wind

- time variant 3D vector field
- turbulence defined along mean wind direction
- inflow angles α_{H}, α_{V}

Reduced wind

- rotor effective wind speed v_0
- wind shears δ_{H}, δ_{V}
- Taylor's Frozen Turbulence Hypothesis

Lidar System Modeling

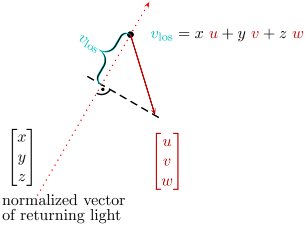

Point measurement model for estimation

- only component in laser beam direction measured
- per convention positive, if towards lidar system

$\rightarrow$ projection of wind vector on normalized laser vector

- if moving: $v_{\mathrm{los}} = x\ (u - \dot{x}_{\mathrm{L}}) + y\ (v - \dot{y}_{\mathrm{L}}) + z\ (w - \dot{z}_{\mathrm{L}})$

Volume measurement model for simulation

- $v_{\mathrm{los}} = \int_{-\infty}^{\infty} (x\ u + y\ v + z\ w)\, f_{\mathrm{rw}}(a)\, \mathrm{d}a$
- pulsed: constant over distance
- continuous wave: increasing with distance^2

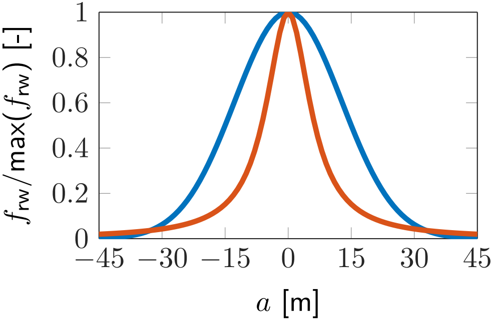

Wind Turbine Modeling

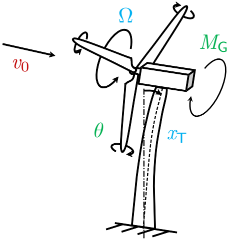

Fatigue, Aerodynamics, Structures, Turbulence (FAST)

- NREL 5 MW (16 DOFs) [1]
- disturbance: 3D turbulent wind field
- aerodynamics: iterative calculation via BEM

$\rightarrow$ sufficiently realistic model for load simulations

Simplified Low Order Wind turbine (SLOW)

- rotor motion Ω and tower motion x_T (2 DOFs) [2]
- rotor effective wind speed v_0
- inputs: blade pitch θ and generator torque M_G

$\rightarrow$ sufficiently accurate model for controller design

Reduced model for controller design

Structural dynamics

rotor motion: $J\dot{\Omega} = M_{\text{a}} - M_{\text{G}} r_{\text{GB}}$

tower motion: $m\ddot{x}_{\text{T}} + c\dot{x}_{\text{T}} + k(x_{\text{T}} - x_{\text{T0}}) = F_{\text{a}}$

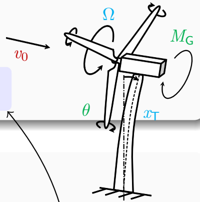

Aerodynamics

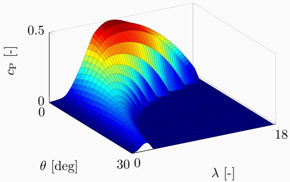

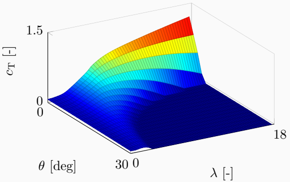

torque: $M_{\text{a}} = \frac{1}{2}\rho\pi R^2 \frac{c_{\text{P}}(\lambda,\theta)}{\Omega} v_{\text{rel}}^3$ thrust: $F_{\text{a}} = \frac{1}{2}\rho\pi R^2 c_{\text{T}}(\lambda,\theta) v_{\text{rel}}^2$

with tip speed ratio $\lambda = \frac{\Omega R}{v_{\text{rel}}}$ and relative wind speed $v_{\text{rel}} = v_0 - \dot{x}_{\text{T}}$

Model Based Wind Field Reconstruction

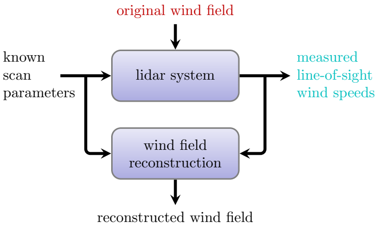

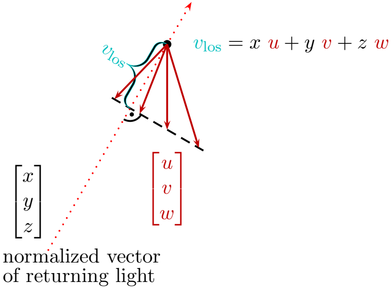

Control engineer's view

- known input
- measurable outputs
- unknown disturbance
- apply observer approach to reconstruct wind

Cyclops Dilemma

- limitation to line-of-sight v_{los}
- we cannot measure u, v, w
- but we can provide estimates with adequate wind models
- depends on application

Application to Ground Based Lidar Systems

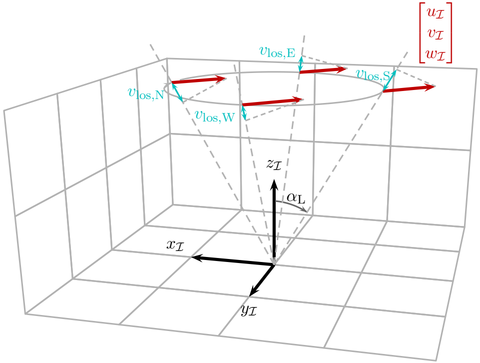

- reconstruction = simulation^{-1}
- solution equal to official equations
- no error if both models are identical

Simulation: Flat terrain → homogeneous flow

$$\underbrace{\begin{bmatrix} v_{\text{los,N}} \\ v_{\text{los,W}} \\ v_{\text{los,S}} \\ v_{\text{los,E}} \end{bmatrix}}_{m} = \underbrace{\begin{bmatrix} \sin\alpha_{\text{L}} & 0 & \cos\alpha_{\text{L}} \\ 0 & \sin\alpha_{\text{L}} & \cos\alpha_{\text{L}} \\ -\sin\alpha_{\text{L}} & 0 & \cos\alpha_{\text{L}} \\ 0 & -\sin\alpha_{\text{L}} & \cos\alpha_{\text{L}} \end{bmatrix}}_{A} \underbrace{\begin{bmatrix} u_{\mathcal{I}} \\ v_{\mathcal{I}} \\ w_{\mathcal{I}} \end{bmatrix}}_{s}$$

Reconstruction: same model

$s = A^{+}m$ with Moore-Penrose pseudoinverse A^{+} solution to least-squares problem

$$\min_{s} \|m - As\|_2$$

$$A^{+} = \begin{bmatrix} \frac{1}{2\sin\alpha_{\text{L}}} & 0 & \frac{-1}{2\sin\alpha_{\text{L}}} & 0 \\ 0 & \frac{1}{2\sin\alpha_{\text{L}}} & 0 & \frac{-1}{2\sin\alpha_{\text{L}}} \\ \frac{1}{4\cos\alpha_{\text{L}}} & \frac{1}{4\cos\alpha_{\text{L}}} & \frac{1}{4\cos\alpha_{\text{L}}} & \frac{1}{4\cos\alpha_{\text{L}}} \end{bmatrix}$$

Application to Ground Based Lidar Systems

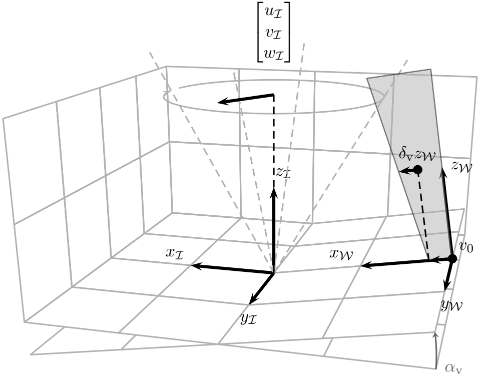

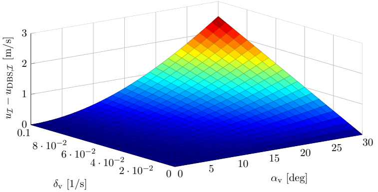

Simulation: inhomogeneous flow (slope)

- simplest “complex” terrain
- vertical inflow angle α_V
- wind homogeneous on in $\mathcal{W}$ system
- vertical linear shear δ_V

Reconstruction: homogeneous flow (DBS)

model discrepancy leads to error

$$u_\mathcal{I} - u_{\mathrm{DBS},\mathcal{I}} = \delta_\mathrm{V} z_\mathcal{I} \sin^2 \alpha_\mathrm{V}.$$

Reconstruction: inhomogeneous flow

- α_V known: no error
- α_V unknown: more heights needed

SWE Scanning Lidar Systems

- Windcube + 2 DOF mirror
- pulsed system, 5 range gates
- can be mounted on nacelle
- main challenge: coordination of mirror and laser

Static Wind Field Reconstruction

$$\underbrace{\begin{bmatrix} v_{\text{los},1} \\ v_{\text{los},2} \end{bmatrix}}_{m} = \underbrace{\begin{bmatrix} x_1 & y_1 \\ x_2 & y_2 \end{bmatrix}}_{A} \underbrace{\begin{bmatrix} u \\ v \end{bmatrix}}_{s}$$

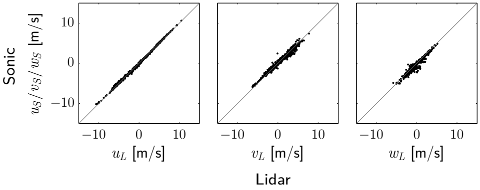

SWE scanner at Risø

- tilted towards met mast
- comparison to sonics
- 10 min averages

Flat terrain

- assuming no w component
- using 2 measurements
- matrix inversion $s = A^{-1}m$

Independent of terrain

- nonlinear wind model using characteristics $v_0, \delta_V, \alpha_V, \alpha_H$
- using 12 measurements
- least square minimization

Application to Floating Lidars

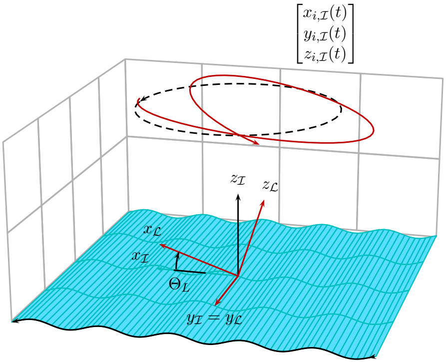

$$\underbrace{\begin{bmatrix} v_{\text{los},1} \\ \vdots \\ v_{\text{los,n}} \end{bmatrix}}_{m} = \underbrace{\begin{bmatrix} x_1 & y_1 & z_1 \\ \vdots & \vdots & \vdots \\ x_n & y_n & z_n \end{bmatrix}}_{A} \underbrace{\begin{bmatrix} u \\ v \\ w \end{bmatrix}}_{s}$$

Calm See

- lidar ($\mathcal{L}$) and inertial ($\mathcal{I}$) coordinate system equal
- normal VAD can be applied
- equal to $s = A^{+}m$ with Moore-Penrose pseudoinverse

With Waves [3]

- lidar ($\mathcal{L}$) and inertial ($\mathcal{I}$) coordinate system different
- inertial coordinates in A from inclination measurements (Θ_L)
- again $s = A^{+}m$ can be applied
- additional correction for lidar system velocity or using nonlinear model with vertical shear might be useful

Coordinate Transformation

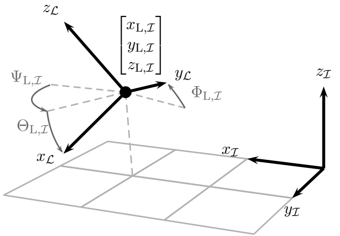

Rotation order from norm for aircraft DIN 9300

yaw Ψ_L $\rightarrow$ pitch Θ_L $\rightarrow$ roll Φ_L, known as $z - y' - x''$.
Other possiblities see [wikipedia.org].

The transformation from the lidar to the inertial coordinate system is

$$\begin{bmatrix} x_{i,\mathcal{I}} \\ y_{i,\mathcal{I}} \\ z_{i,\mathcal{I}} \end{bmatrix} = \boldsymbol{T}_{\mathcal{I}\mathcal{L}} \begin{bmatrix} x_{i,\mathcal{L}} \\ y_{i,\mathcal{L}} \\ z_{i,\mathcal{L}} \end{bmatrix} + \begin{bmatrix} x_{\mathsf{L},\mathcal{I}} \\ y_{\mathsf{L},\mathcal{I}} \\ z_{\mathsf{L},\mathcal{I}} \end{bmatrix} \quad \text{with}$$

$$\boldsymbol{T}_{\mathcal{I}\mathcal{L}} = \underbrace{\begin{bmatrix} \cos(\Psi_\mathsf{L}) & -\sin(\Psi_\mathsf{L}) & 0 \\ \sin(\Psi_\mathsf{L}) & \cos(\Psi_\mathsf{L}) & 0 \\ 0 & 0 & 1 \end{bmatrix}}_{T_\text{yaw}} \underbrace{\begin{bmatrix} \cos(\Theta_\mathsf{L}) & 0 & \sin(\Theta_\mathsf{L}) \\ 0 & 1 & 0 \\ -\sin(\Theta_\mathsf{L}) & 0 & \cos(\Theta_\mathsf{L}) \end{bmatrix}}_{T_\text{pitch}} \underbrace{\begin{bmatrix} 1 & 0 & 0 \\ 0 & \cos(\Phi_\mathsf{L}) & -\sin(\Phi_\mathsf{L}) \\ 0 & \sin(\Phi_\mathsf{L}) & \cos(\Phi_\mathsf{L}) \end{bmatrix}}_{T_\text{roll}}$$

Lidar-Data-Processing for Floating Lidars

Measurement Equation

$$v_{\mathsf{LOS}} = x_{\mathcal{I}}(u_{\mathcal{I}} - \dot{x}_{\mathsf{L},\mathcal{I}}) + y_{\mathcal{I}}(v_{\mathcal{I}} - \dot{y}_{\mathsf{L},\mathcal{I}}) + z_{\mathcal{I}}(w_{\mathcal{I}} - \dot{z}_{\mathsf{L},\mathcal{I}})$$

v_{LOS}	scalar line-of-sight speed provided by lidar
$u_{\mathcal{I}}, v_{\mathcal{I}}, w_{\mathcal{I}}$	wind velocity at focal point in inertial coordinate system $\mathcal{I}$
$x_{\mathcal{I}}, y_{\mathcal{I}}, z_{\mathcal{I}}$	beam vector in inertial coordinate system $\mathcal{I}$
$\dot{x}_{\mathsf{L},\mathcal{I}}, \dot{y}_{\mathsf{L},\mathcal{I}}, \dot{z}_{\mathsf{L},\mathcal{I}}$	lidar system velocity measured by IMU in inertial coordinate system $\mathcal{I}$

Motion compensation

$$\begin{aligned} v_{\mathsf{LOS,mc}} &= v_{\mathsf{LOS}} + x_{\mathcal{I}}\dot{x}_{\mathsf{L},\mathcal{I}} + y_{\mathcal{I}}\dot{y}_{\mathsf{L},\mathcal{I}} + z_{\mathcal{I}}\dot{z}_{\mathsf{L},\mathcal{I}} \\ &= x_{\mathcal{I}}u_{\mathcal{I}} + y_{\mathcal{I}}v_{\mathcal{I}} + z_{\mathcal{I}}w_{\mathcal{I}} \end{aligned}$$

- beam vector from IMU‘s rotational DOFs and beam vector in lidar coordinate system $\mathcal{L}$
- now $v_{\mathsf{LOS,mc}}$ can be used as before

Main Idea [4]

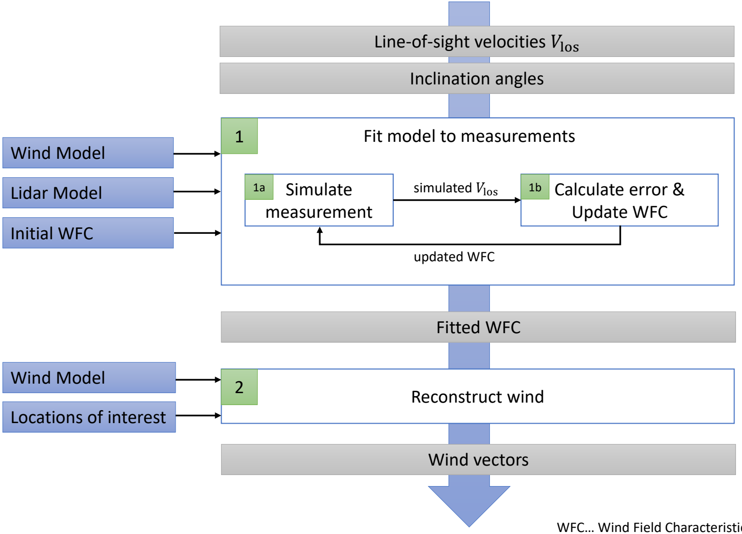

WFC... Wind Field Characteristics

Wind Field Reconstruction in the Induction Zone

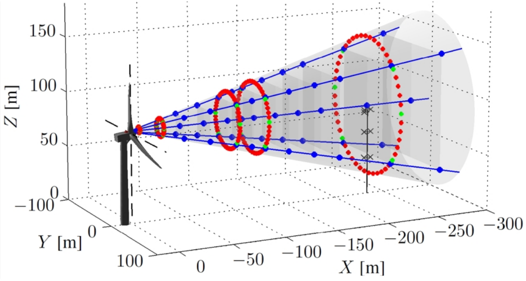

[5]

Benefits

- measurement closer to the turbine can be used
- impact of complex terrain can be reduced

Main idea [5]

- include induction zone model into WFR
- estimate induction zone model parameter together with other wind field characteristics

1D Induction Zone Model [6]

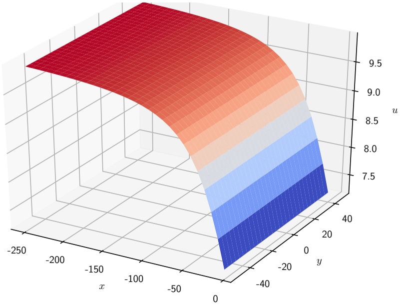

$$u(x) = v_\infty \left(1 - a\left(1 + \frac{x/R}{\sqrt{1+(x/R)^2}}\right)\right)$$

v_∞	free wind speed
a	induction factor

Wind Field Reconstruction in the Induction Zone - Results [5]

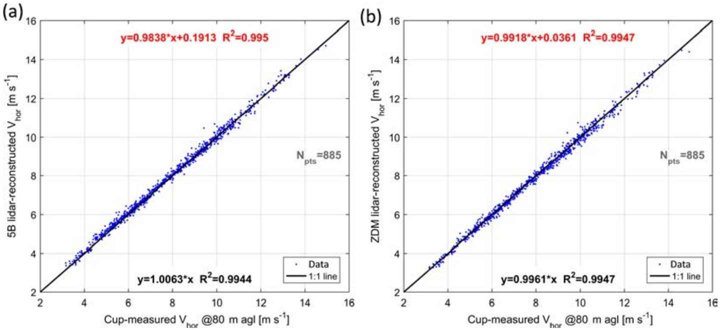

Figure 9. Comparison between mast-measured and lidar-estimated horizontal wind speed at hub height and $2.5D_{\mathrm{rot}}$ using short-range measurements. **(a)** 5B-Demo lidar, using five LOS and four ranges. **(b)** ZDM lidar, using six LOS and three ranges.

Data filtering		Reconstruction case		Forced linear regressions results			
Case	Direction sector	Dataset	Lidar	Input measurement ranges	Gain	R^2	Number of periods
1	$[93°, 123°]$	Joint	5B-Demo, 5 LOS	$2.0\ D_{\mathrm{rot}}$	1.0146	0.9936	885
			ZDM, 6 LOS	$2.5\ D_{\mathrm{rot}}$	1.0090	0.9938	
			5B-Demo, 5 LOS	from 0.5 to 1.15 D_{rot}	1.0063	0.9944	
			ZDM, 6 LOS	from 0.3 to 1.25 D_{rot}	0.9961	0.9947	

Dynamic Wind Field Reconstruction

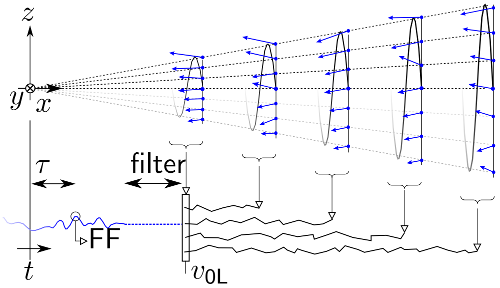

Adjustments for control

- nacelle- and spinner-based
- high temporal resolution
- synchronized with control
- overall effect to rotor

Rotor-effective wind speed v_{0L}

- combination to one signal
- assuming perfect alignment
- using frozen turbulence

Signal is then usually filtered and used in the feedforward (FF) controller with a preview time τ before the wind hits the rotor to overcome actuator reaction time.

More Complex Dynamic Wind Field Reconstruction

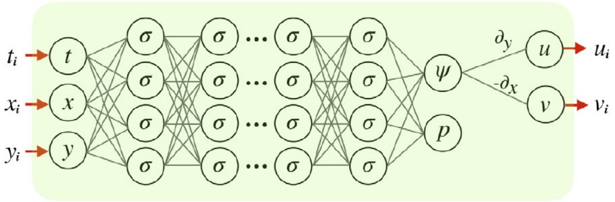

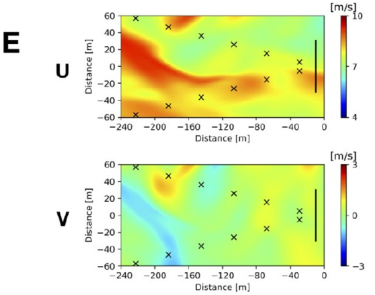

[7]

Approaches using Navier-Stokes-Equations

- Unscented Kalman-Filter using simplified dynamic model based on NS [8]
- Training of physics-informed deep learning models using LES simulations [7]
- Wind-field characterization using proper orthogonal decomposition [9]

Rotor-effective Wind Speed from Turbine Data

Using a wind turbine as anemometer

$$J\dot{\Omega} = M_\mathrm{a} - M_\mathrm{G} r_\mathrm{GB}$$

$$\frac{\Omega R}{v_0}$$

$$\frac{1}{2}\rho\pi R^2 \frac{c_\mathrm{P}(\lambda,\theta)}{\Omega} v_0{}^3$$

- unknown rotor-effective wind speed
- measurable turbine data

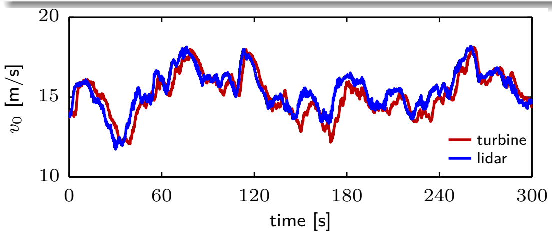

Comparison over time

- preview visible
- larger trends similar
- smaller details differ

Correlation Model - Understanding Wind Preview Quality

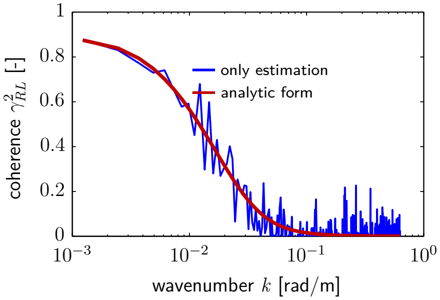

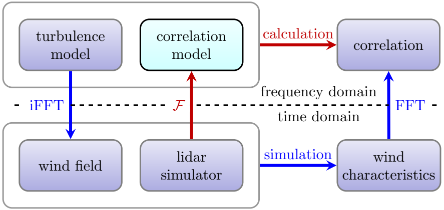

We can directly calculate how well a lidar system measures!

Coherence γ^2_{RL}

- between $v_{0\mathrm{L}}$ and v_0
- no(0)$\rightarrow$perfect(1) correlation
- wavenumber $\sim 1/$(eddy size)
- bandwidth $k_{0.5}$ at $\gamma^2_{\mathrm{RL}} = 0.5$

Time domain simulation

- lidar simulator
- time consuming

Frequency domain calculation

- Fourier transform
- fast and automated

Correlation Model - Approach [10, 11]

Coherence is defined by

$$\gamma_{\mathrm{RL}}^2 = \frac{|S_{\mathrm{RL}}|^2}{S_{\mathrm{RR}} S_{\mathrm{LL}}}.$$

Auto-spectrum of $v_0 = \frac{1}{n}\sum_{i=1}^{n} u_i$

$$\begin{aligned} S_{\mathrm{RR}} &= \mathcal{F}\{v_0\}\mathcal{F}^*\{v_0\} \\ &= \frac{1}{n^2}\sum_{i=1}^{n}\sum_{j=1}^{n} \underbrace{\mathcal{F}\{u_i\}\mathcal{F}^*\{u_j\}}_{S_{ij,u}} \\ &= \frac{S_{ii,u}}{n^2}\sum_{i=1}^{n}\sum_{j=1}^{n}\gamma_{ij,u} \end{aligned}$$

spectra $S_{ii,u}$ and coherence $\gamma_{ij,u}$ from turbulence model, e.g. Kaimal

Cross-spectrum of v_0 and $v_{0\mathrm{L}}$

$$S_{\mathrm{RL}} = \mathcal{F}\{v_0\}\mathcal{F}^*\{v_{0\mathrm{L}}\}$$

Auto-spectrum of $v_{0\mathrm{L}}$

$$S_{\mathrm{LL}} = \mathcal{F}\{v_{0\mathrm{L}}\}\mathcal{F}^*\{v_{0\mathrm{L}}\}$$

expressed by u, v, w spectra and coherences including effects of:

- temporal/spatial averaging
- discrete scanning
- wind field reconstruction
- wind evolution

- coherence can be modeled by auto- and cross-spectra
- based on Fourier transform of measurement equations

Adaptive Filter Design

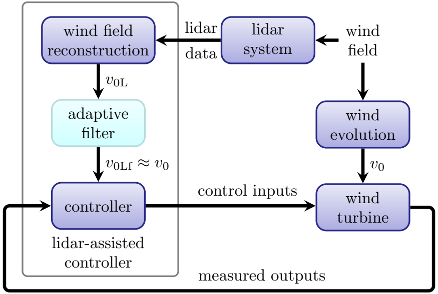

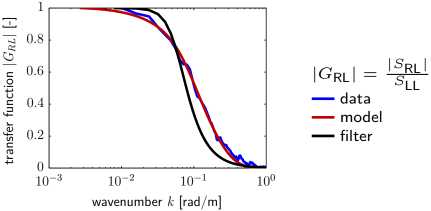

Why do we need a filter?

- controller is designed assuming perfect wind preview, so we match v_{0L} to v_0
- to filter out all uncorrelated frequencies to avoid harmful and unnecessary control action

How can we design a filter?

- transfer function from v_{0L} to v_0
- from data or model
- fit of linear filter
- changes with mean wind speed
- or use Wiener filter [12]

Lidar System Optimization

$$\max_{n_P, r, x_1} \quad k_{0.5}$$

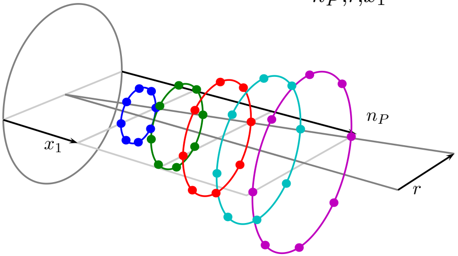

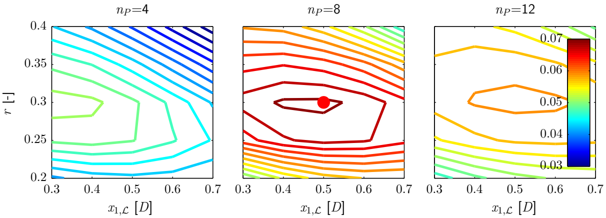

Optimization problem

- SWE-lidar on NREL 5 MW
- best coherence bandwidth $k_{0.5}$
- number of points n_P
- first distance x_1
- normalized radius r

Solution

- optimal setup ●
- found by brute force

Classifications of Lidar Systems for Control [13]

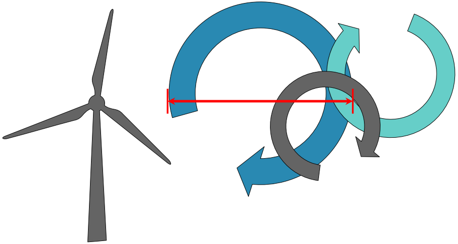

Smallest Detectable Eddy Size

- turbulence structure still detectable by a lidar
- simplified: inverse of coherence bandwidth
- can be normalized by rotor diameter D
- $1D$ very good, $1.5D$ good
- $2D$ average, $3D$ sufficient

Short Exercise 1

Task 1: Measurement equations

A lidar systems measures at $[40, 30, 0]$ m where the wind vector is $[u, v, w]$. What is the line-of-sight wind speed signal?

Solution 1

$$v_{\text{los}} = \frac{4}{5}\,u + \frac{3}{5}\,v.$$

Task 2: Spectrum

With given auto-spectra S_{uu} and S_{vv}, and given cross-spectrum $S_{uv} = 0$: What is the line-of-sight wind speed spectrum?

Solution 2

$$S_{\text{los}} = \frac{16}{25}\,S_{uu} + \frac{9}{25}\,S_{vv}.$$

Short Exercise 2

Task 1: Cut-off-frequency

A lidar systems measures at 100 m. The transfer function from the rotor-effective wind speed estimate of the lidar to the one estimated from turbine data reaches - 3dB at a wave number of 0.02 rad/m for 25 m/s. What should be the cut-off-frequency of a first order low pass?

Solution 1

$$f_{\text{cut-off}} = \frac{0.5}{2\pi}\text{Hz}.$$

Task 2: Buffer time

Scan time is 1 s, pitch actuator reaction time is 0.4 s, filter delay is 1.4 s. How much time do you need to buffer the signal?

Solution 2

$$T_{\text{buffer}} = \frac{100}{25}\text{s} - 0.5\text{s} - 1.4\text{s} - 0.4\text{s} = 1.7\text{s}.$$

Conclusions

Main questions

- How can useful wind preview signals be extracted from lidar data?

Nacelle-based lidar needs new model-based wind field reconstruction!

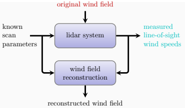

- Main problem: limitation to line-of-sight wind speeds.
- Good estimates can be provided with adequate wind models!
- For lidar-assisted control we can assume perfect alignment and the Frozen Turbulence Hypothesis to condense all line-of-sight to an estimate for the rotor-effective wind speed.

Correlation between lidar and rotor very important!

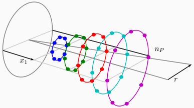

- Rotor-effective wind speed can be also estimated from turbine data.
- We can model spectra, transfer function and coherence based on Fourier transform of measurement equations and using turbulence models.
- Lidar data needs to be filtered according to the transfer function.
- We can use the correlation model for scan optimization and filter design.

References I

[1] J. Jonkman, S. Butterfield, W. Musial, and G. Scott. *Definition of a 5-MW Reference Wind Turbine for Offshore System Development*. Tech. rep. TP-500-38060. NREL, 2009. DOI: 10.2172/947422.

[2] D. Schlipf. “Lidar-Assisted Control Concepts for Wind Turbines”. PhD thesis. University of Stuttgart, 2015. DOI: 10.18419/opus-8796.

[3] F. Kelberlau, V. Neshaug, L. Lønseth, T. Bracchi, and J. Mann. “Taking the motion out of floating lidar: Turbulence intensity estimates with a continuous-wave wind lidar”. In: *Remote Sensing* 12.5 (2020), p. 898. DOI: 10.3390/rs12050898.

[4] D. Schlipf, A. Rettenmeier, F. Haizmann, M. Hofsäß, M. Courtney, and P. W. Cheng. “Model based wind vector field reconstruction from lidar data”. In: *German Wind Energy Conference (DEWEK)*. Bremen, Germany, Nov. 2012. DOI: 10.18419/opus-8136.

References II

[5] A. Borraccino, D. Schlipf, F. Haizmann, and R. Wagner. "Wind field reconstruction from nacelle-mounted lidar short-range measurements". In: *Wind Energy Science* 2.1 (May 2017), pp. 269–283. DOI: 10.5194/wes-2-269-2017.

[6] A. R. Meyer Forsting, N. Troldborg, A. Bechmann, and P.-E. Réthoré. "Modelling Wind Turbine Inflow: The Induction Zone". PhD thesis. Technical University of Denmark, 2017. DOI: 10.11581/DTU:00000022.

[7] J. Zhang and X. Zhao. "Spatiotemporal wind field prediction based on physics-informed deep learning and LIDAR measurements". In: *Applied Energy* 288 (2021), p. 116641. DOI: https://doi.org/10.1016/j.apenergy.2021.116641.

[8] P. Towers and B. L. Jones. "Real-time wind field reconstruction from LiDAR measurements using a dynamic wind model and state estimation". In: *Wind Energy, published online* (2014).

References III

[9] E. S. Sagredo, J. Rinker, S. Andersen, and J. Forrest. "Wind-field characterization using synthetic lidar measurements and proper orthogonal decomposition". In: *Journal of Physics: Conference Series* (2024). The Science of Making Torque from Wind (TORQUE 2024).

[10] D. Schlipf, J. Mann, and P. W. Cheng. "Model of the correlation between lidar systems and wind turbines for lidar-assisted control". In: *Journal of Atmospheric and Oceanic Technology* 30.10 (Oct. 2013), pp. 2233–2240. DOI: 10.1175/jtech-d-13-00077.1.

[11] D. P. Held and J. Mann. "Lidar estimation of rotor-effective wind speed – an experimental comparison". In: *Wind Energy Science* 4.3 (2019), pp. 421–438. DOI: 10.5194/wes-4-421-2019.

[12] E. Simley and L. Y. Pao. "Reducing LIDAR wind speed measurement error with optimal filtering". In: *Proceedings of the American Control Conference*. Washington, DC, USA, 2013. DOI: 10.1109/ACC.2013.6579906.

References IV

[13] D. Schlipf, H. Fürst, S. Raach, and F. Haizmann. "Systems engineering for lidar-assisted control: a sequential approach". In: *Journal of Physics: Conference Series*. Vol. 1102. WindEurope conference 2018 within the Global Wind Summit. Hamburg, Germany, Sept. 2018, p. 012014. DOI: 10.1088/1742-6596/1102/1/012014.

Please let me know if you have further questions!

Prof. Dr.-Ing. David Schlipf
David.Schlipf@HS-Flensburg.de
www.hs-flensburg.de/go/WETI

Disclaimer